Paull, C.K., Matsumoto, R., Wallace, P.J., and Dillon, W.P. (Eds.), 2000
Proceedings of the Ocean Drilling Program, Scientific Results, Vol. 164

7. ISOTOPIC COMPOSITION OF CH_4, CO_2 SPECIES, AND SEDIMENTARY ORGANIC MATTER WITHIN SAMPLES FROM THE BLAKE RIDGE: GAS SOURCE IMPLICATIONS[1]

C.K. Paull,[2,3] T.D. Lorenson,[4] W.S. Borowski,[2,5] W. Ussler III,[2] K. Olsen,[2,6] and N.M. Rodriguez[2,5]

ABSTRACT

The isotopic characteristics of CH_4 ($\delta^{13}C$ values range from –101.3‰ to –61.1‰ PDB, and δD values range from –256‰ to –136‰ SMOW) collected during Ocean Drilling Program (ODP) Leg 164 indicate that the CH_4 was produced by microbial CO_2 reduction and that there is not a significant contribution of thermogenic CH_4 to the sampled sediment gas from the Blake Ridge. The isotopic values of CO_2 ($\delta^{13}C$ range –20.6‰ to +1.24‰ PDB) and dissolved inorganic carbon (DIC; $\delta^{13}C$ range –37.7‰ to +10.8‰ PDB) have parallel profiles with depth, but with an offset of 12.5‰. Distinct downhole variations in the carbon isotopic composition of CH_4 and CO_2 cannot be explained by closed-system fractionation where the CO_2 is solely derived from the locally available sedimentary organic matter ($\delta^{13}C$ –2.0‰ ± 1.4‰ PDB) and the CH_4 is derived from CO_2 reduction. The observed isotopic profiles reflect the combined effects of upwards gas migration and decreased microbial activity with depth.

INTRODUCTION

Background

Ocean Drilling Program (ODP) Leg 164 was devoted to investigating amounts and in situ characteristics of natural gas hydrates contained in marine sediments. Sites 994, 995, and 997 were drilled along a ~10-km-long transect across the crest of the Blake Ridge (Fig. 1) to depths of 700–750 mbsf. A well-developed bottom simulating reflector (BSR) occurs under Sites 995 and 997, whereas Site 994 has no underlying BSR. Sites 994, 995, and 997 were drilled through the depth of the acoustically detected BSR (~450 m). Four short-hole sites (total depth of 49–63 mbsf) were also drilled along the flanks and crest of the Cape Fear (Sites 991, 992, and 993) and Blake Ridge diapirs (Site 996; Fig. 1; Paull, Matsumoto, Wallace, et al., 1996).

Gas hydrate nodules were recovered, the largest of which was a ~30-cm-thick horizon of massive gas hydrate. Shipboard gas hydrate decomposition experiments revealed that evolved gases are composed of ~99% CH_4 and ~1% CO_2 (Lorensen et al., Chap. 25, this volume).

Sediments from the three deep sites (Sites 994, 995, and 997) and Site 996 are very gassy and undergo vigorous expansion during core recovery. Because gas hydrates actively decompose during core recovery and the curation process, and because obvious gas loss occurs before sampling, various proxy measurements are used to define the in situ distributions of gas and gas hydrate. Pore-water profiles from the three sites show freshening of chloride to depths of ~200 mbsf. From 200 to 450 mbsf, chloride concentrations are highly variable, and characterized by local, anomalous excursions toward lower values. These anomalies indicate that variations of up to 14% in the amount of gas hydrate contained in adjacent samples occur throughout this zone and that finely disseminated gas hydrates, on average, occupy more than 1% of the sedimentary section between 200 and 450 mbsf at all three sites, regardless of whether a BSR is present (Sites 995 and 997) or not (Site 994). Well logs show distinct zones of higher electrical resistivity and sonic velocity that coincide with chloride anomaly occurrences (Collett and Ladd, Chap. 19, this volume). Vertical seismic profiles indicate that the velocity of sediments above the BSR are not significantly elevated above normal sediment velocities. However, acoustic velocities as low as 1400 m/s were measured immediately beneath the BSR at Site 997 (Holbrook et al., 1996) and are attributed to the accumulation of free gas.

Methane gas volumes measured using the ODP pressure core sampler (PCS) tool are in excess of in situ CH_4 gas saturation in pore water, demonstrating that free gas exists intermittently throughout the sedimentary section below the base of gas hydrate stability. PCS data indicate that the amount of free gas in the sediments beneath the base of gas hydrate stability may exceed the volume stored in the hydrates above (Dickens et al., 1997).

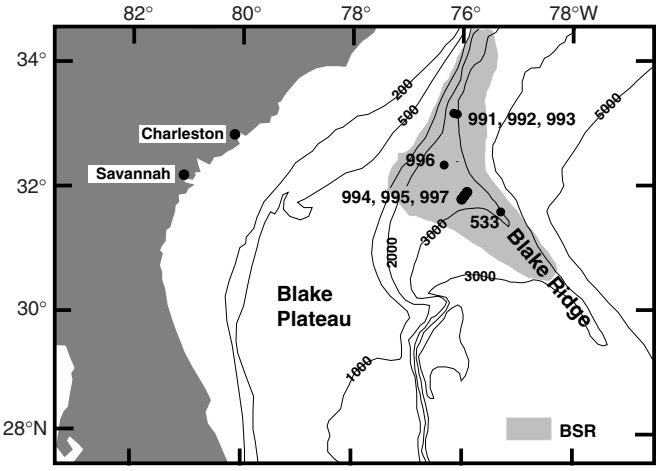

Figure 1. Map showing the location of ODP Leg 164 sites (Sites 991–997) and DSDP Site 533 with respect to the regional BSR (Paull, Matsumoto, Wallace, et al., 1996).

[1]Paull, C.K., Matsumoto, R., Wallace, P.J., and Dillon, W.P. (Eds.), 2000. *Proc. ODP, Sci. Results,* 164: College Station, TX (Ocean Drilling Program).
[2]Geology Department, University of North Carolina, Chapel Hill, NC 27599-3315, U.S.A.
[3]Present address: Monterey Bay Aquarium Research Institute, 7700 Sandholdt Road, Moss Landing, CA 95039-0628, U.S.A. paull@mbari.org
[4]Pacific Marine Geology, U.S. Geological Survey, Menlo Park, CA 94025, U.S.A.
[5]Present address: Exxon Exploration Company, P.O. Box 4778, Houston, TX 77210-4778, U.S.A.
[6]Present address: Marine Sciences, State University of New York, Stony Brook, NY 11794, U.S.A.

The results of Leg 164 confirm that marine gas hydrates and the associated dissolved and gaseous phases represent a major methane reservoir. In this paper, we consider the origins of interstitial CH_4 and associated interstitial CO_2 and their relationship to sedimentary organic matter.

Sources of Interstitial Low Molecular-Weight Hydrocarbon Gases and CO_2

In normal marine sediments, distinct sequences of microbial zones occur with sediment burial that influence methane accumulation. In the upper portion of the sedimentary section, microbial CH_4 production is at first inhibited by the presence of sulfate (Martens and Berner, 1974). Neither significant CH_4 production nor accumulation will occur until the sulfate is substantially depleted. Microbial CH_4 production commences near the base of the sulfate-reduction zone, usually resulting in increasing pore-fluid CH_4 concentrations with increasing depth. This effect is caused by local CH_4 production and the addition of CH_4, which migrates from greater depths. If CH_4 comes from greater depths, either by diffusion or advection, it may have been produced by either microbial processes or thermal hydrocarbon cracking (Tissot and Welte, 1984).

Methane

Microbial methane is produced primarily by CO_2 reduction ($CO_2 + 4H_2 \rightarrow CH_4 + 2H_2O$) and acetate fermentation ($CH_3COOH \rightarrow CH_4 + CO_2$) with CO_2 reduction primarily dominate in marine systems (Fenchel and Blackburn, 1979). CO_2 reduction is dependent on a supply of dissolved H_2, whereas acetate fermentation is usually limited by the amount of acetate available. Both limiting reactants are derived in part from the breakdown of larger organic molecules comprising sedimentary organic matter. Considerable carbon isotope fractionation (commonly 60‰–70‰) is associated with methanogenesis (e.g., Rosenfeld and Silverman, 1959; Whiticar et al., 1986).

Thermogenic methane is produced as a consequence of thermocatalytic degradation of kerogen at temperatures over ~120°C (Tissot and Welte, 1984), which, with typical geothermal gradients, requires burial depths significantly greater than ~1 km. Because less fractionation occurs during thermal cracking of kerogen (Schoell, 1983), the carbon isotopic composition of CH_4 produced from thermal cracking of kerogen is closer to the carbon isotopic composition of its parent sedimentary organic matter.

Interstitial CO_2

Interstitial dissolved CO_2 may be derived from organic sources, which include anaerobic oxidation of organic matter, and abiogenic thermal decarboxylation reactions (Claypool and Kaplan, 1974). The isotopic composition of the CO_2 that is added to the dissolved inorganic carbon (DIC) pore-water pool by these processes will reflect that of the organic matter from which it is derived (Presley and Kaplan, 1968). Carbon in the DIC pool may also be supplied from inorganic sources, primarily carbonate dissolution. The isotopic composition of carbon from dissolution of biogenic carbonate rarely varies more than a few parts per million (~2 ppm) from 0‰ (Anderson and Arthur, 1983).

Dissolved CO_2 sinks include methanogenesis (CO_2 reduction) and authigenic carbonate formation (Rodriguez et al., Chap. 30, this volume). Authigenic carbonates are precipitated at or near isotopic equilibrium with the dissolved pore-water species (Anderson and Arthur, 1983). However, methanogenesis preferentially uses $^{12}CO_2$ to form methane, shifting the remaining CO_2 pool toward enriched $\delta^{13}C$ values.

Low Molecular-Weight Hydrocarbon Gases

The ratio of low molecular-weight hydrocarbon gases (e.g., methane/ethane ratio) and $\delta^{13}C_{CH_4}$ values are commonly used to establish the methane's source. Microbial CH_4 typically has $\delta^{13}C_{CH_4}$ values that range from –90‰ to –55‰ (PDB) and methane to ethane ratios of >1000 (Bernard et al., 1977). Thermogenic CH_4 typically has $\delta^{13}C_{CH_4}$ values more positive than –55‰ and methane to ethane ratios less than 100 (Bernard et al., 1977). In addition, δD_{CH_4} values are used to distinguish between the two major microbial methane-production pathways (Schoell, 1980; Whiticar et al., 1986). The hydrogen in CH_4 comes solely from surrounding water if the CH_4 has been produced by CO_2 reduction, whereas three-fourths of the hydrogen in CH_4 comes from organic matter and only one-fourth from water if the CH_4 is produced by acetate fermentation. Thus, in natural systems, CH_4 produced via acetate fermentation characteristically has δD values more negative than –250‰ SMOW), with typical values between –355‰ and –290‰, whereas CH_4 produced from CO_2 reduction is characterized by δD values more positive than –250‰ with typical values near –191‰ ± 19‰ (Whiticar et al., 1986).

Organic Matter Base Line

In marine sediments, the source for CH_4 and CO_2 carbon is typically sedimentary organic matter. Thus, to understand variations in the isotopic composition of these mobile carbon phases in a sedimentary sequence, it is necessary to establish the elemental and isotopic composition of the organic matter and to document any significant stratigraphic changes in the parental organic matter. Although only a small fraction of the original organic matter in an ancient sediment may survive, the isotopic composition of the remaining organic matter in the host sediments is believed to faithfully reflect the original organic matter source (Meyers, 1994).

Characteristically, the $\delta^{13}C$ and $\delta^{15}N$ composition of bulk sedimentary organic matter depends on whether the carbon and nitrogen came from the atmosphere or seawater, and on the specific biochemical pathways. Tropospheric CO_2 carbon is ~7‰ (Wahlen et al., 1993), whereas marine bicarbonate is ~0‰ (Anderson and Arthur, 1983). The carbon fractionation associated with the most common photosynthetic pathway (C3 pathway) is ~–20‰ (Deines, 1980). Terrestrial organic matter typically has $\delta^{13}C$ values more negative than –24‰, whereas marine organic matter typically has values more positive than –23‰ (Meyers, 1994). Similarly, $\delta^{15}N$ values of bulk sedimentary organic matter are also indicative of the source: values more positive than 7‰ indicate marine sources, and values more negative than 3‰ are characteristic of terrestrial sources (Cifuentes et al., 1988).

The C:N value of organic matter also reflects its source. Typically marine algae have atomic C:N values between 4 and 10, whereas organic matter produced by terrestrial plants (C3 and C4 pathways), typically have C:N values that exceed 20 (Meyers, 1994).

Previous Work on Blake Ridge Methane Sources

Deep Sea Drilling Project (DSDP) Sites 102, 103, 104, and 533 were also drilled on the Blake Ridge (Shipboard Scientific Party, 1972; Gradstein and Sheridan, 1983). Isotopic measurements of the CO_2 gas, DIC, CH_4, and organic carbon were reported in unprecedented detail from Site 533 to the depth of 399 mbsf (Brooks et al., 1983; Claypool and Threlkeld, 1983; Galimov and Kvenvolden, 1983). ODP Leg 164 extends the isotopic stratigraphies initially outlined at Site 533 to greater depths (~750 mbsf) and to other sites along the Blake Ridge.

METHODS

Gas samples were collected during Leg 164 using four different techniques:

1. Free gas samples were extracted by inserting a piercing tool through the core liner and into sediment voids. At shallow depths free core gas was extracted from the core liner by opening a valve to an evacuated container connected to a hypodermic needle. Below about 50 mbsf, the gas within the voids generally escaped under its own pressure into a 60-cm^3 syringe.
2. Short sections of core were sealed in gas collection tubes to collect the gases that evolved from core sections as the cores warmed within the core laboratory (Paull, Matsumoto, Wallace, et al., 1996). Selected core sections (cut into the standard 1.5-m-long lengths on the catwalk) were placed in 1.54-m-long tubes that were slightly larger in diameter than the core liners. The tubes were constructed from standard PVC schedule-40 pipe sections (ID ~3.5 in) with end caps that were machined so that they would seal on both ends with O-ring-fitted plates that could be bolted on quickly to make a gas-tight seal. Holes were drilled in the core liners just before the cores were sealed in the tube to let gas escape. Thus, all the gas that evolved within the core after they were sealed in the tubes could be collected and analyzed. Gas from each core flowed out one end of a gas collection tube through tygon tubing into an overturned 1-L graduated cylinder, floating in a bath filled with NaCl-saturated water. Because the cylinders were initially water filled, the volume of water displaced by the gas could be measured directly and sampled through luer-lock fittings by 60-cm^3 syringes.
3. The pressure core sampler (PCS) is a downhole tool that seals a small diameter sediment core in an internal chamber at in situ pressure. Upon recovery, the gases within the sealed PCS were vented in a stepwise fashion (Dickens et al., 1997), and aliquots of the gas were collected for compositional and isotopic analysis.
4. Gas samples were collected from five solid gas hydrate samples that were individually placed in a sealed chamber, quickly evacuated, and allowed to dissociate within the closed vessel (Lorenson et al., Chap. 25, this volume).

Relative concentrations of methane, carbon dioxide, and major low molecular-weight hydrocarbon gases (ethane, propane, and butane) were measured on shipboard by gas chromatograph (Paull, Matsumoto, Wallace, et al., 1996). The remaining gas was transferred underwater into inverted 20-mL glass vials, sealed with a rubber stopper, and crimp-sealed with aluminum caps for transport and storage.

$\delta^{13}C$ values of CH_4 and CO_2 were measured with a Finnigan MAT 252 gas-chromatograph-isotope-ratio-mass-spectrometer (GC-IR-MS) at the University of North Carolina-Chapel Hill (UNC-CH) using the methods of Merritt and Hayes (1995) and Popp et al. (1995). The results of 251 CH_4 and 137 CO_2 gas analyses are reported in Tables 1 and 2. Twelve samples contained enough ethane for $\delta^{13}C$ measurements (Table 3).

Forty-one CH_4-bearing samples were analyzed for their hydrogen isotope composition (Table 4). Methane was separated using a cryogenic vacuum line and combusted to CO_2 and water. The water was converted to H_2 gas in a reaction with hot zinc and captured in glass break seals (Coleman et al., 1982; Kendall and Coplen, 1985; Hayes and Johnson, unpubl. data). δD measurements were made with a Finnigan MAT 252 mass spectrometer at UNC-CH.

Pore-water samples were stored in flame-sealed glass ampoules for shore-based isotopic measurement of total DIC. DIC within pore-water samples was separated and collected using standard, cryogenic vacuum line techniques (Craig, 1953). Carbon isotope measurements were made on 105 samples (Table 5) using a Delta E mass spectrometer at North Carolina State University.

The bulk organic fraction in 58 sediment samples was analyzed for $\delta^{13}C$, $\delta^{15}N$, and C:N values (Table 6) using a technique modified from Hedges and Stern (1984). Residual solid phase samples from the shipboard pore-water extraction were broken, and ~50-g pieces from the interior were subsampled and placed in precombusted Pyrex beakers. The samples were freeze dried and then crushed with a mortar and pestle. Dry, powdered samples were placed in a vapor chamber containing 12N hydrochloric acid for 24 hr to remove the inorganic carbon fraction. This technique works well for samples that contain less than 20% $CaCO_3$; samples with more than 20% $CaCO_3$ are not reported here because of incomplete $CaCO_3$ digestion. Subsamples were combusted within a Carlo Erba C/N elemental analyzer and passed directly through the Finnigan MAT 252 GC-IR-MS at UNC-CH providing a $\delta^{13}C$ and $\delta^{15}N$ value for each sample. Chromatographic peak areas were used to calculate the atomic C:N value for each sample.

Isotopic values are reported with respect to PDB for $\delta^{13}C$, SMOW for δD, and air for $\delta^{15}N$ values. The cumulative (vacuum line, preparation, and mass spectrometer) accuracy of isotopic measurements are +0.2‰ for $\delta^{13}C_{CO_2}$, $\delta^{13}C_{CH_4}$, $\delta^{13}C_{DIC}$, $\delta^{13}C_{Org.\,C}$, $\delta^{13}C_{C_2H_6}$, and $\delta^{15}N_{Org.\,C}$, and +3‰ for δD_{CH_4} (Neal Blair and Howard Mendlovitz, pers. comm., 1997). However, because these samples have experienced obvious degassing, we suspect that the intersample variations inherent in the sampling methods far exceed the laboratory errors for the various gas measurements.

RESULTS

Methane Isotopes

The 251 $\delta^{13}C$ analyses of CH_4 samples collected on Leg 164 have a mean of –68.4‰ ± 7.0‰ and range between –101.3‰ and –61.1‰ (Table 1). The stratigraphic profiles of $\delta^{13}C_{CH_4}$ values are indistinguishable between Sites 994, 995, and 997 (Fig. 2). At these three sites, $\delta^{13}C_{CH_4}$ values become more positive with depth from a minimum of –101.3‰ (21.45 mbsf, Site 995) near the top of the methane-bearing zone to a stable value of –64.0‰ ± 0.9‰ (n = 65) between 300 mbsf and the bottom of the holes (at 700–750 mbsf). The rate of change in the CH_4 profile is highest near the top of the CH_4-bearing zone.

Forty-one analyses of δD of the selected CH_4 samples have a mean value of –187‰ ± 20‰ (Table 5). No stratigraphic variation in the δD values is discernible. No variation in CH_4 isotopic values occurs near the base of gas hydrate–bearing sediments (~450 mbsf) at these sites (Paull, Matsumoto, Wallace, et al., 1996).

Five gas samples were measured that came directly from decomposing gas hydrate (Table 1). The isotopic composition of this CH_4 is indistinguishable from nearby gas samples collected by other methods. The isotopic composition of the CH_4 samples obtained from the PCS is separately considered in a companion paper (Wallace et al., Chap. 10, this volume).

The two $\delta^{13}C_{CH_4}$ measurements available from Sites 991 (40.6 mbsf) and 993 (27.5 mbsf; Fig. 2) plot near the trend outlined by gases from Sites 994, 995, and 997. In contrast, the 21 measurements of $\delta^{13}C_{CH_4}$ from Site 996 range from –72.1‰ to –62.5‰ with a mean value of –68.38‰ ± 1.9‰. These samples do not follow the same depth trend seen at Sites 994, 995, and 997 (Fig. 2), but rather are similar to the values that occur below 200 mbsf at Sites 994, 995, and 997.

Table 1. $\delta^{13}C$ composition of methane and carbon dioxide in gas samples collected from Leg 164 cores.

Core, section	Depth (mbsf)	$\delta^{13}C$ (CH_4) (‰ PDF)	$\delta^{13}C$ (CO_2) (‰ PDB)	Type
164-991A-				
5H-3	40.60	–72.4	–25.8	GT
164-993A-				
4X-4	27.50	–77.4	–30.3	GT
164-994C-				
6H-3	45.10	–81.9	–18.2	GT
6H-3	45.10	–81.8	–20.2	GT
7H-3	54.90	–81.7	–10.7	GT
8H-3	64.40	–76.2	–8.9	GT
8H-5	67.40	–75.9	–8.2	GT
10H-1	71.90	–76.6		GT
11H-3	84.40	–75.2	–7.1	GT
12H-3	93.90	–76.8		GT
13H-2	101.90	–74.5	–7.6	GT
14H-4	114.40	–72.7	–6.6	GT
15H-2	120.26	–72.4	–4.2	GT
16H-3	131.90	–73.1	–5.3	GT
17H-4	142.90	–72.2	–2.0	GT
22X-2	176.40	–71.2	–4.4	
30X-5	246.83	–68.1	–5.3	GT
31X-7	260.75	–63.5	–5.7	GH
52X-1	424.50	–63.8	–9.2	GT
68X-4	554.10	–63.3		FG
69X-4	564.51	–63.0	–13.4	FG
71X-2	575.10	–63.3	–13.4	FG
72X-2	580.80	–64.7	–12.0	FG
79X-2	646.88	–62.7	–15.5	GT
79X-4	650.68	–63.9	–16.5	FG
80X-5	661.21	–63.5	–15.2	FG
81X-5	670.64	–63.7	–16.5	FG
84X-3	697.60	–65.0	–18.2	FG
164-994D-				
1H-1	100.00	–71.1		GT
1H-1	100.00	–73.2		GT
1H-2	101.50	–71.9		GT
1H-2	101.50	–71.6		GT
1H-3	103.00	–73.4		GT
1H-3	103.00	–74.1		GT
1H-3	103.00	–74.9		GT
1H-4	104.50	–73.2		GT
1H-4	104.50	–73.6		GT
1H-5	106.00	–73.1		GT
1H-5	106.00	–71.5		GT
1H-5	106.00	–72.6		GT
1H-5	106.00	–72.9		GT
164-995A-				
12H-2	89.13	–74.6	–5.2	FG
12H-6	95.18	–74.1	–4.9	FG
14H-2	109.20	–73.9	–4.8	FG
14H-3	110.70		–5.3	FG
15H-6	124.70	–71.8	–2.5	FG
16H-5	131.58	–70.6	–4.1	FG
19H-4	150.58	–69.1	–1.1	FG
41X-1	339.50	–64.8	–7.5	FG
42X-2	350.60	–64.8	–6.6	FG
43X-1	358.70	–64.5	–7.7	FG
44X-2	369.90	–64.0	–6.5	FG
53X5	433.10	–63.6	–10.0	FG
55X-1	445.40	–64.5	–11.0	FG
57X-2	466.20	–63.2	–10.3	FG
65X-2	533.60	–62.7	–12.2	FG
67X-3	554.30	–62.2	–13.6	FG
68X-5	566.90	–62.3	–11.6	FG
69X-4	573.50	–63.2	–14.9	FG
71X-3	583.34	–62.4	–15.1	FG
78X-1	647.40	–63.9		FG
79X-2	657.82	–62.8	–15.9	FG
80X-3	669.15	–63.5	–15.9	FG
81X-3	679.20	–63.6	–16.1	FG
82X-3	687.88	–63.6	–18.1	FG
83X-4	699.90	–63.8	–17.4	FG
164-995B-				
6X-1	245.10	–67.0	–5.0	FG
8X-3	312.88	–66.5	–6.7	FG
12X-2	419.80	–63.9	–8.8	FG
13X-3	430.90	–63.7	–8.0	FG
15X-3	450.10	–63.3	–9.8	FG
2H	17.20	–79.6		PW
2H	20.02	–93.3		PW
2H	20.23	–93.9		PW
2H	20.63	–95.4		PW
2H	21.25	–98.5		PW
2H	21.44	–101.3		PW
2H	21.75	–97.5		PW
2H	22.13	–93.6		PW
2H	22.33	–92.3		PW
2H	22.63	–90.3		PW
2H	22.83	–90.7		PW
164-996A-				
8H-4 (1)	50.93	–62.5	–14.5	GT
8H-4 (2)	50.93	–67.3	–8.9	GT
8H-4	50.93	–69.1	–21.9	GT
8H-4	52.50	–69.3	–23.2	FG
9H-CC	63.00	–67.4	–19.9	FG
9H-CC	63.00	–67.8	–18.5	FG
164-996D-				
1H-1	1.14	–66.6	–22.3	FG
1H-2	0.02	–65.8	–26.9	FG
4H-1	23.18	–72.1	–11.4	GT
6H-1	42.28	–68.0	–14.6	GT
6H-2	43.05	–69.5	–5.3	GT
9H-6	49.05	–67.3	–14.7	GT
164-996E-				
7H-CC	52.90	–70.7	–21.9	FG
164-997A-				
7H-1	50.50	–76.6	–8.2	FG
8H-2	54.50	–77.8	–17.5	FG
9H-1	61.50	–79.3	–12.7	FG
10H-7	79.85	–74.7	–5.1	FG
11H-3	83.50	–74.1	–5.7	FG
12H-6	97.42	–73.4	–5.2	FG
13H-7	107.58	–72.3	–1.6	FG
22X-4	176.82	–68.3	–3.4	FG
26X-5	209.50	–66.2	–2.0	FG
27X-4	216.60	–67.7	–2.1	FG
28X-2	223.20	–66.5	–2.8	FG
30X-3	235.40	–66.6	–2.3	FG
41X-3	321.80	–65.0	–4.4	FG
42X-3	330.50	–65.8	–21.1	FG
43X-1	337.10	–65.0	–6.5	FG
44X-4	351.30	–64.9	–7.0	FG
46X-4	370.25	–64.9		FG
48X-2	386.90	–64.6	–8.3	FG
52X-5	413.10	–63.8	–6.7	FG
54X-4	427.98	–65.4	–8.6	FG
164-997B-				
1X-2	320.10	–65.6	–5.4	FG
2X-2	329.70	–66.1	–5.3	FG
4X-1	414.30	–65.5		FG
5X-2	425.66	–65.0	–8.3	FG
8X-5	449.00	–64.3	–11.4	FG
11X-3	446.30	–64.5	–9.0	FG
12X-3	474.21	–64.8	–11.3	FG
13X-3	484.60	–63.9	–11.5	FG
14X-2	492.70	–64.2	–10.4	FG
16X-3	504.90	–63.6	–12.3	FG
17X-1	510.50	–63.9	–11.6	FG
18X-2	521.60	–63.9	–11.1	FG
19X-3	532.70	–63.6	–11.7	FG
20X-1	539.30	–63.1	–12.2	FG
22X-4	554.40	–63.2	–13.1	FG
23X-6	566.00	–63.6	–13.5	FG
24X-4	572.60	–64.0	–17.2	FG
26X-4	583.20	–63.3	–17.2	FG
27X-5	593.20	–63.4	–15.9	FG
28X-4	600.70	–63.8	–16.0	FG
29X-3	609.60	–63.6	–14.2	FG
30X-3	619.20	–64.3	–17.0	FG
31X-4	630.23	–63.9	–15.7	FG
33X-4	640.07	–63.8	–16.5	FG
34X-1	645.00	–62.4		FG
35X-5	658.80	–64.3	–17.0	FG
37X-5	671.20	–63.7	–16.8	FG
38X-5	679.90	–64.1	–16.6	FG
42X-3	704.77	–64.4	–18.8	FG
43X-4	716.80	–64.3	–17.5	FG
45X-4	727.26	–64.1	–16.2	FG
46X-4	734.84	–64.3	–17.1	FG
47X-4	745.70	–64.4	–17.9	FG
164-997A-				
4H-3	34.90	–84.0	–20.6	GT
5H-3	34.90	–82.4	–19.3	GT
6H-3	44.40	–80.8	–15.6	GT
10H-3	74.30	–75.2	–7.4	GT
14H-4	112.73	–71.2	–1.2	GT
15H-3	121.90	–71.1	–1.1	GT
16H-3	131.40	–70.9	0.8	GT
16H-3	131.40	–71.3	1.1	GT
22X-3	176.00	–69.2	–0.9	GT
35X-3	272.95	–69.0	–2.2	GT

Note: GT = gas tube samples, FG = free gas samples, PW = pore water, GH = gas hydrate samples. Numbers in ( ) = the number of the analyzed gas aliquot from a given PCS core.

Table 2. $\delta^{13}C$ composition of methane and carbon dioxide in gas samples collected from the pressure core sampler during Leg 164.

Core, section	Depth (mbsf)	$\delta^{13}C$ (CH_4) (‰ PDB)	$\delta^{13}C$ (CO_2) (‰ PDB)
164-994C-			
27P (2)	223.50	–67.0	–22.7
27P (3)	223.40	–67.9	–9.1
36P (2)	300.40	–61.1	–18.2
66P	541.10	–64.3	–12.1
70P	569.90	–63.0	–20.1
164-995A-			
27P (1)	222.90	–71.3	–3.9
27P (2)	222.90	–67.7	–5.1
27P (3)	222.90	–68.2	–9.5
27P (5)	222.90	–69.3	–10.4
27P (6)	222.90	–68.4	–5.9
36P (1)	300.30	–71.4	–18.6
36P (2)	300.30	–65.9	–16.8
36P (3)	300.30	–66.0	–10.3
36P (4)	300.30	–65.0	–9.2
45P (1)	377.50	–73.5	–32.5
45P (6)	377.50	–64.9	–32.7
45P [132 psi]	377.50	–63.9	–11.8
45P (25)	377.50	–63.9	–8.9
48P (1)	396.80	–65.0	–27.0
48P (2)	396.80	–65.0	–23.2
48P (3)	396.80	–63.9	–17.0
48P (4)	396.80	–63.4	–23.1
60P (1)	493.10	–67.3	–27.9
60P (2)	493.10	–65.2	–22.1
60P (3)	493.10	–64.2	–21.3
60P (4)	493.10	–63.4	–28.3
70P	579.60	–63.9	–16.9
164-995B-			
7P (6B)	308.5	–65.3	–9.0
7P (7B)	308.5	–65.1	–5.9
7P (9)	308.5	–68.2	–22.7
7P (13)	308.5	–65.8	–21.9
7P (14)	308.5	–68.8	–27.2
7P (15)	308.5	–68.6	–27.2
7P (18)	308.5	–68.8	–24.2
7P (20)	308.5	–68.6	–22.5
164-996A-			
7P (3)	48.00	–69.4	–28.6
7P (4)	48.00	–69.3	–30.3
7P (6)	48.00	–68.7	–28.4
7P (8)	48.00	–68.8	–32.7
7P (16)	48.00	–68.0	–28.3
7P (17)	48.00	–68.4	–27.0
7P (19)	48.00	–68.4	–24.8
7P (22)	48.00	–70.6	–25.1
7P (24)	48.00	–68.5	–25.9
164-996D-			
7P (5)	52.00	–69.1	–29.8
7P (7)	52.00	–68.0	–28.4
7P (9)	52.00	–68.3	–24.4
7P (10)	52.00	–69.3	–29.8
7P (11)	52.00	–66.0	–27.2
7P (12)	52.00	–66.8	–24.5
7P (13)	52.00	–66.3	–21.1
7P (14)	52.00	–67.6	–31.4
7P (15)	52.00	–67.6	–26.6
164-997A-			
25P (1)	202.40	–69.1	
25P (2)	202.40	–68.4	
25P (3)	202.40	–67.9	
25P (4)	202.40	–67.3	
33P (1)	260.10	–66.6	
33P (2)	260.10	–66.9	
40P	317.70	–65.7	
49P (1)	394.90	–62.4	
49P (2)	394.90	–64.1	
49P (3)	394.90	–64.0	
49P (4)	394.90	–64.8	
49P (5)	394.90	–64.3	
49P (6)	394.90	–64.2	
49P (7)	394.90	–64.6	
49P (8)	394.90	–64.2	
49P (9)	394.90	–64.7	
49P (10)	394.90	–64.7	
55P (1)	433.30	–64.7	
55P (2)	433.30	–64.1	
55P (3)	433.30	–64.0	
55P (4)	433.30	–64.3	
55P (6)	433.30	–64.9	
55P (7)	433.30	–63.9	
55P (9)	433.30	–63.6	
164-997B-			
10P (3)	462.20	–63.3	
10P (4)	462.20	–63.5	
10P (5)	462.20	–63.2	
10P (6)	462.20	–64.6	
10P (7)	462.20	–63.0	
10P (8)	462.20	–64.4	
10P (9)	462.20	–63.5	
10P (10)	462.20	–63.2	
10P (11)	462.20	–65.0	
15P (2)	501.80	–64.4	
15P (3)	501.80	–63.1	
15P (4)	501.80	–63.4	
15P (5)	501.80	–65.5	
15P (6)	501.80	–63.2	
15P (7)	501.80	–64.9	
21P (1)	549.90	–64.3	
21P (2)	549.90	–64.2	
21P (3)	549.90	–63.1	
21P (4)	549.90	–63.0	
21P (5)	549.90	–62.7	
21P (6)	549.90	–63.3	
21P (7)	549.90	–62.8	
21P (8)	549.90	–62.0	
29P (1)	549.90	–65.1	
29P (2)	549.90	–62.8	
32P (1)	606.50	–63.3	
36P (1)	664.10	–64.1	
36P (2)	664.10	–63.7	
40P (1)	693.00	–64.2	
44P (1)	721.80	–64.3	

Note: Numbers in ( ) = the number of the analyzed gas aliquot from a given PCS core.

Table 3. $\delta^{13}C$ values of ethane in gas samples from Site 997.

Sample identification	Depth (mbsf)	$\delta^{13}C$ (‰ PDB)
997A-27	216	–69.4
997B-2	329	–67.6
997A-44	351	–66.9
997A-52	413	–66.7
997B-5	425	–66.2
997B-13	484	–66.5
997B-17	510	–66.8
997B-22	554	–65.5
997B-27	593	–63.5
997B-31	630	–63.4
997B-37	671	–63.3
997B-45	727	–62.3

Ethane Isotopes

The 12 measurements of $\delta^{13}C_{C_2H_6}$ values (Table 3) range from –69.4‰ at 216 mbsf to –63.3‰ at 727 mbsf, with a mean value of –65.7‰ ± 2‰. The values change linearly (R = 0.95) with depth.

$\delta^{13}C$ of CO_2 Gas and DIC

At Sites 994, 995, and 997 the $\delta^{13}C$ values of gaseous CO_2 samples ranged from –20.6‰ to +1.24‰, whereas the $\delta^{13}C_{DIC}$ values ranged from –37.7‰ to +10.8‰. The $\delta^{13}C$ values of the CO_2 gas and the DIC samples are generally parallel but offset by ~12.5‰ (Fig. 2).

The stratigraphic variations in carbon isotopic composition of both the CO_2 in the gas that evolved from the cores (and the parallel values of the measured DIC) reveal distinct depth zones (Fig. 3). DIC $\delta^{13}C$ values in the upper 40 mbsf show a sharply defined minimum at ~20 mbsf (Figs. 2, 3). Above this level there is an approximately linear change in the DIC $\delta^{13}C$ values that roughly corresponds with a mixing line between overlying seawater DIC ($\delta^{13}C$ = ~0) and the very ^{13}C depleted values at 20 mbsf (e.g., 37.7‰ at Site 995). Below ~20 mbsf the DIC $\delta^{13}C$ values become more positive. The increase over the interval between 20 and 40 mbsf is the most rapid and is almost symmetrical with the decrease occurring over the first 20 mbsf (Fig. 3). Below 20 mbsf the $\delta^{13}C$ values increase slowly before reaching a maximum between 120 and 150 mbsf. Below 150 mbsf, the $\delta^{13}C$ trend of both the DIC and CO_2 gas reverses and linearly (or perhaps

Table 4. δD and $\delta^{13}C$ composition of selected methane samples.

Core, section	Depth (mbsf)	δD (‰ SMOW)	$\delta^{13}C$ (‰ PDB)
164-994C-			
5H-4	38.90	–183	–80.6
6H-3	45.10	–187	–81.8
8H-3	64.40	–178	–76.6
5H-4	38.90	–183	–80.6
14H-5	117.30	–183	–68.1
17H-4	141.40	–190	–64.3
25X-2	550.30	–185	–67.7
30X-3	244.00	–191	–68.1
40X-2	331.00	–138	–71.8
41X-4	341.77	–178	–69.8
50X-1	406.70	–180	–69.6
50X-2	407.00	–198	–61.6
62X-3	513.80	–200	—
67X-2	542.50	–175	–67.5
80X-5	661.21	–203	–63.5
81X-5	670.64	–195	–63.7
164-996B-			
1H*	0.20	–200	—
164-996D-			
1H*	0.20	–136	–65.8
1H*	0.20	–175	–66.6
4H-1	23.18	–191	—
9H-6	49.05	–192	—
164-996E-			
7H-CC*	52.90	–193	–70.7
164-997A-			
5H-3	34.90	–256	–82.4
9H-6	74.00	–181	–73.0
13H-7	107.58	–166	–72.3
13H-7	107.58	–196	–72.3
16H-3	131.00	–186	—
18P-1	147.00	–187	–67.8
22X-4	216.60	–184	–64.8
28X-2	386.90	–190	–66.5
41X-3	321.80	–196	–65.0
42X-3*	331.00	–191	–65.8
48X-2	386.90	–181	–64.6
54X-4	427.98	–150	–65.4
164-997B-			
8X-4	448.80	–165	–59.7
12X-3	474.21	–230	–64.5
14X-2	492.00	–189	–64.2
15P	501.80	–183	–64.4
18X-2	521.60	–197	–63.9
37X-1	665.50	–195	–61.6
47X-4	745.70	–201	–64.4
47X-4	745.70	–192	–64.4

Note: * = gas hydrate sample. — = no data.

asymptotically) converges to within ~3‰ of the organic carbon values at the base of the holes.

Site 996 has isotopically distinct CO_2 gas and DIC profiles from those at the deeper sites. The most negative value of $\delta^{13}C_{DIC}$ (–45.0‰) occurred at a shallow depth of 3.72 mbsf at Site 996 (Fig. 3). The mean of the eight samples with sub-bottom depths less than 10 mbsf is –38.65‰ ± 4.5‰, whereas the samples below 28 mbsf have a mean value of 5.5‰ ± 6.7‰. The isotopic composition of the carbonates from Site 996 is considered in Naehr et al. (Chap. 29, this volume).

Organic Carbon Characteristics

Values of $\delta^{13}C$ of bulk organic carbon at Sites 994, 995, and 997 range between –19.7‰ and –25.4‰, with a mean value of –22.0‰ ± 1.4‰ (Fig. 2; Table 6). $\delta^{15}N$ values of the same sedimentary organic matter samples range from 3.2‰ to 6.8‰ with a mean value of 5.6‰ ± 0.7‰ (Table 6). The mean value for the C:N value in all these samples is 8 ± 2 (Table 6). Although the values in the upper hundred meters show more scatter, no significant stratigraphic trends are revealed by these data.

DISCUSSION

Bulk Organic Matter Composition

Measurements of the isotopic values of both $\delta^{13}C$ and $\delta^{15}N$ contained in the organic matter in the Blake Ridge sediments at Sites 994, 995, and 997 characterize the source of the sedimentary organic matter. Mean $\delta^{13}C$ values (–22.0‰ ± 1.4‰) and $\delta^{15}N$ values (5.6‰ ± 0.7‰), plus the low C:N values (8 ± 2), indicate that the source of the sedimentary organic matter is largely marine (Meyers, 1994).

The stratigraphic uniformity of the organic carbon profile defines a constant baseline (i.e., –22.0‰ ± 1.4‰) for the organic carbon pool. The lack of significant stratigraphic variation in the $\delta^{13}C$ (Fig. 2), $\delta^{15}N$, and C:N values of bulk sedimentary organic carbon sampled from Blake Ridge sediments indicates that the character of the organic matter supplied to the Blake Ridge has not changed significantly throughout the sections sampled at Sites 994, 995, and 997. The variation in the isotopic composition of the host organic carbon is too small to be a major factor in generating the observed isotopic changes in the CH_4 and dissolved CO_2 pools.

Offset Between $\delta^{13}C$ Values of CO_2 Gas and DIC

A significant isotopic offset (~12.5‰) exists between the $\delta^{13}C$ values of CO_2 gas and DIC. A similar offset (~10‰) was reported between these pools at DSDP Site 533 (Claypool and Threlkeld, 1983). The offset is presumed to be an artifact of CO_2 outgassing during sediment recovery. A significant equilibrium carbon isotope fractionation (8.38 ± 0.12‰, at 20°C; Emrich et al., 1970) occurs between bicarbonate and gaseous CO_2. However, the observed $\delta^{13}C$ offset is larger than equilibrium predicts.

Gas phases are only generated when saturation occurs during core recovery, largely as a consequence of the large decrease in pressure between the subseafloor and the surface. Because CH_4 (Duan et al., 1992), but not CO_2 (Weiss, 1974), becomes supersaturated as these cores are recovered, the majority of the original CH_4 in the sediments below ~100 mbsf is lost during the core-recovery process (Dickens, et al., 1997). In fact, comparisons between the volume of gas in PCS samples and traditional headspace gas measurements below 300 mbsf indicate that ~99% of the original CH_4 escapes during the recovery process. We infer that the DIC pool is sparged during CH_4 degassing, and thus much of the original in situ DIC pool is lost as CO_2 gas. A consequence of this loss is that the DIC and CO_2 gas pools become fractionated relative to each other. Thus, the measured pore-water DIC isotope values reflect the residual DIC in the pore water after vigorous degassing and fractionation and not the isotopic composition of the original DIC pool.

The $\delta^{13}C_{DIC}$ values should accurately reflect the composition of the in situ DIC pool until CH_4 saturation occurs (~30 mbsf). Below this level the original (predegassing) $\delta^{13}C$ values of the DIC pool probably lie somewhere between the measured CO_2 gas and DIC values, but closer to the CO_2 gas values, because these samples may more accurately reflect the majority of the original gas volume. In this paper, DIC $\delta^{13}C$ values are used to describe the changes in the CO_2 pool in the upper 50 mbsf (the approximated depth at which visually obvious degassing started), and $\delta^{13}C$ values of CO_2 gas are used below this level.

Origin of In Situ DIC

The distinct minimum of DIC carbon isotopic composition at ~20 mbsf is believed to be associated with a zone of active anaerobic methane oxidation (AMO; Reeburgh, 1976, 1980). This minimum corresponds with the sulfate-methane interface (Borowski et al., 1997). Within this AMO zone, ^{13}C-depleted carbon obtained from CH_4 oxidation is added to the DIC pool. Consequently, ^{13}C-depleted DIC has diffused both upward and downward, depressing the $\delta^{13}C$

Table 5. $\delta^{13}C$ values of dissolved inorganic carbon (DIC) samples from pore waters collected on Leg 164.

Core, section	Depth (mbsf)	$\delta^{13}C$ (‰ PDB)
164-994A-		
1H-1	1.40	–13.0
1H-3	4.40	–18.2
2H-1	9.30	–27.5
2H-3	12.30	–31.4
2H-5	15.30	–33.6
3H-1	18.80	–36.1
3H-2	20.30	–37.2
3H-3	21.80	–35.0
3H-5	24.80	–28.1
4H-2	28.89	–18.8
164-994C-		
4H-4	31.89	–17.6
4H-6	34.89	–11.6
5H-5	40.35	–4.3
6H-4	48.05	0.5
7H-4	57.85	2.6
10H-2	74.80	5.4
12H-2	93.80	7.7
17H-3	142.80	9.7
22X-5	180.80	10.6
24X-1	194.95	9.5
30X-2	244.60	8.0
38X-1	310.45	6.3
44X-1	368.15	5.0
49X-5	402.67	4.2
54X-3	439.50	3.8
56X-2	456.25	2.8
61X-2	495.75	1.4
71X-2	571.75	–1.3
75X-4	613.25	–1.9
84X-2	696.60	–4.8
164-994D-		
9X-5	412.75	5.8
164-995A-		
8H-5	66.10	4.3
11H-3	82.29	6.7
13H-5	105.20	9.2
17H-5	143.10	9.9
24X-1	195.35	9.7
28X-3	228.65	8.8
35X-3	295.00	6.8
42X-1	349.90	5.5
46X-3	382.39	4.1
49X-4	403.60	3.6
51X-2	418.80	5.3
54X-2	438.00	3.7
55X-1	446.20	3.6
56X-1	455.80	3.1
61X-6	500.34	0.4
71X-4	585.64	–3.5
78X-1	647.95	–2.0
83X-7	703.80	–3.7

Core, section	Depth (mbsf)	$\delta^{13}C$ (‰ PDB)
164-995B-		
1H-1	0.38	–5.1
1H-3	4.08	–16.5
1H-5	7.40	–22.5
2H-1	17.40	–36.1
2H-2	18.90	–37.0
2H-3	20.40	–37.7
2H-4	21.90	–35.8
2H-5	23.40	–31.5
164-995A-		
5H-5	37.65	–9.9
6H-5	47.10	–1.7
164-996A-		
1H-1	0.85	–42.3
1H-6	3.62	–36.1
3X-1	10.11	–28.4
8H-2	49.61	10.5
9H-3	61.55	10.1
164-996B-		
1H-3	2.44	–32.5
164-996D-		
1H-1	0.00	–40.3
1H-1	0.20	–37.0
4H-7	28.59	–6.7
6H-2	42.99	10.4
164-996E-		
1H-3	3.72	–45.0
2H-2	6.95	–33.0
2H-4	9.94	–41.5
4H-5	29.05	4.8
6X-6	50.86	3.5
164-997A-		
3H-5	19.80	–30.8
3H-6	21.30	–31.2
4H-1	23.30	–26.0
6H-2	43.80	–1.7
9H-2	64.30	5.3
12H-2	92.80	8.9
17H-5	144.70	10.8
26X-4	209.25	9.9
32X-5	257.80	8.8
39X-5	315.35	6.6
52X-1	406.75	5.2
54X-4	429.13	3.5
164-997B-		
8X-2	445.75	3.0
11X-3	467.45	3.1
16X-4	507.55	1.3
20X-3	543.45	–0.8
28X-2	598.82	–2.2
35X-3	659.95	–5.0
45X-4	728.41	–4.0

values significantly below the organic carbon baseline (–22‰). The processes that occur at the sulfate-methane interface are treated in greater detail elsewhere (Borowski et al., 1997, and Chap. 9, this volume).

The $\delta^{13}C$ value of the shallowest CO_2 gas sample from Site 994 (34.9 mbsf, –20.6‰) is slightly ^{13}C enriched compared to the sedimentary organic carbon base line. From this level down to ~120 mbsf, the $\delta^{13}C$ values of CO_2 gas shift toward increasing ^{13}C enrichment. The observed maximum in $\delta^{13}C$ values of both CO_2 gas and DIC between 120 and 150 mbsf (Fig. 2) requires addition of carbon with an isotopic composition enriched in ^{13}C, and/or preferential subtraction of ^{13}C-depleted carbon relative to the sedimentary organic carbon.

Although biogenic carbonates are enriched in ^{13}C with respect to organic carbon (Rodriguez et al., Chap. 30, this volume), it is unlikely that the addition of carbon from the dissolution of biogenic carbonate is responsible for the ^{13}C enrichment in the dissolved CO_2 pool. The $\delta^{13}C$ value of the CO_2 gas never gets more enriched than biogenic carbonate carbon (~0‰–2‰), but does converge with the biogenic value. Thus, if biogenic carbonate was the source for the depleted carbon, the majority of the carbon in the CO_2 gas would need to have come from biogenic carbonate dissolution. In contrast, the $\delta^{13}C$ values in the DIC samples are significantly enriched over the biogenic carbonate; thus their values cannot be explained by biogenic carbonate dissolution. Furthermore, carbonate textures and the pore-water chemistry suggest that carbonate precipitation, rather than dissolution, is occurring in this interval (Rodriguez et al., Chap. 30, this volume).

The ^{13}C enrichment in the CO_2 pool probably results from fractionation of the dissolved CO_2 pool during CH_4 formation by CO_2 reduction. The residual CO_2 pool becomes ^{13}C enriched as ^{12}C-enriched DIC is selectively removed to form CH_4 by CO_2 reduction (Whiticar et al., 1986). Thus, the observed shift in the $\delta^{13}C$ values and resulting minimum at 120–150 mbsf is consistent with CH_4 formation via CO_2 reduction as previously inferred at Site 533 (Claypool and Threlkeld, 1983; Galimov and Kvenvolden, 1983).

Microbial Origin of Methane and Ethane

We interpret the low molecular-weight hydrocarbon gases recovered during Leg 164 to be produced primarily by microbially mediated CO_2 reduction. All the measured CH_4 samples have $\delta^{13}C_{CH_4}$

Table 6. $\delta^{13}C$ and $\delta^{15}N$ values of sedimentary organic matter from Sites 994, 995, and 997 (after Olsen, 1997).

Core, section	Depth (mbsf)	$\delta^{13}C$ (‰ PDB)	$\delta^{15}C$ (‰ air)	$CaCO_3$ (%)	C/N	Organic carbon (%)
164-994C-						
6H-4	48.05	–20.8	4.45	16.2	6.8	1.9
7H-4	57.85	–9.8	4.68	18.9	9.2	2.3
17H-3	142.85	–22.6	5.72	11.3	6.4	1.4
22X-5	180.80	–21.8	5.31	8.4	10.5	1.0
24X-1	194.95	–21.4	5.21	6.5	8.6	0.8
30X-2	244.65	–21.6	5.84	13.8	9.0	1.7
38X-1	310.45	–21.3	6.49	14.2	10.2	1.7
44X-1	368.15	–21.9	6.04	14.8	7.9	1.8
49X-5	402.67	–21.1	6.08	18.9	9.9	2.3
164-994D-						
9X-5	412.75	–21.3	5.92	16.0	8.5	1.9
164-994C-						
54X-3	439.50	–21.4	6.40	19.2	7.8	2.3
56X-2	456.25	–21.5	6.25	6.8	7.4	0.8
71X-2	572.75	–22.2	6.53	11.1	6.9	1.3
75X-4	613.05	–20.9	6.16	9.9	9.2	1.2
84X-2	696.60	–21.7	5.29	14.4	8.0	1.7
164-995B-						
2H-3	20.40	–9.7	5.48	18.9	5.2	2.3
2H-4	20.80	–21.7	5.04	17.9	2.7	2.2
164-995A-						
5H-5	37.65	–23.4	3.89	6.1	4.4	0.7
7H-5	143.10	–21.8	5.48	18.3	7.6	2.2
24X-1	195.35	–22.1	5.17	11.1	8.7	1.3
28X-3	228.25	–22.9	5.84	5.2	6.5	0.6
35X-3	295.00	–22.0	5.59	11.9	9.9	1.4
36P	300.39	–21.6	5.30	14.8	8.8	1.8
42X-1	349.90	–22.0	5.91	18.6	8.0	2.2
46X-3	382.39	–21.8	5.74	12.5	10.9	1.5
49X-3	403.60	–22.0	5.92	18.8	6.9	2.3
51X-2	418.80	–21.7	6.14	17.4	10.2	2.1
55X-1	446.20	–22.1	6.05	19.6	9.1	2.3
61X-6	500.34	–21.7	6.02	12.1	8.5	1.4
71X-4	585.64	–21.6	6.62	12.4	8.5	1.5
78X-1	647.95	–21.7	5.91	12.2	9.3	1.5
83X-7	703.80	–22.5	5.67	11.3	7.1	1.4
164-997A-						
2H-5	10.30	–24.1	4.12	19.5	3.4	2.3
3H-3	16.80	–21.1	5.47	18.3	7.8	2.2
3H-5	19.80	–23.5	5.00	19.1	4.8	2.3
3H-6	21.30	–22.4	4.52	8.0	4.3	1.0
6H-2	43.80	–25.4	4.97	9.4	5.4	1.1
9H-2	64.30	–24.2	4.72	19.5	5.0	2.3
12H-2	92.80	–22.8	4.44	13.3	16.0	1.6
17H-5	144.70	–22.8	5.31	10.5	10.3	1.3
21X-2	169.80	–23.2	5.27	10.2	10.6	1.2
26X-4	209.25	–23.4	5.49	12.3	9.1	1.5
30X-1	233.60	–23.1	5.18	14.9	10.7	1.8
32X-5	257.80	–23.3	5.33	15.5	10.4	1.9
39X-5	315.35	–23.0	5.25	13.6	40.4	1.6
52X-1	406.75	–21.3	5.37	17.1	9.7	2.1
54X-4	429.13	–21.4	6.17	14.5	8.9	1.7
164-997B-						
8X-2	445.75	–21.5	6.40	7.1	10.4	0.9
11X-3	467.45	–21.8	6.05	12.6	9.5	1.5
14X-2	493.60	–21.4	6.84	13.1	12.0	1.0
16X-4	507.55	–21.2	6.26	13.9	10.7	1.7
20X-3	543.45	–21.6	6.12	10.7	9.2	1.3
28X-2	598.82	–21.7	6.50	11.6	9.0	1.4
29X-4	612.60	–21.5	6.08	8.0	7.9	1.0
35X-3	659.95	–20.7	5.60	12.2	8.5	1.5
39X-3	687.70	–21.1	5.98	18.6	9.2	2.2
45X-4	728.41	–20.8	5.76	15.5	11.0	1.9

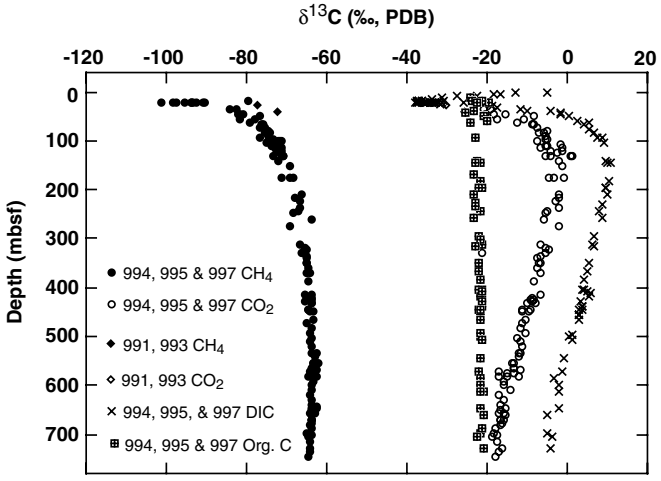

Figure 2. Profiles of carbon isotopic values of methane and carbon dioxide in the free gases, dissolved inorganic carbon (DIC), and bulk sedimentary organic carbon for Sites 991, 993, 994, 995, and 997 vs. sub-bottom depth. Symbols are indicated in key. Data are in Tables 1, 2, 5, and 6.

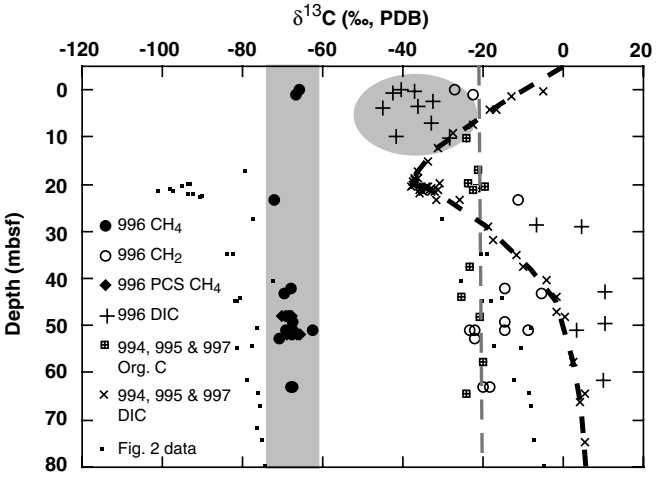

Figure 3. Profiles of carbon isotopic values of methane and carbon dioxide in the free gases, PCS-collected methane, and dissolved inorganic carbon (DIC) in Site 996 vs. sub-bottom depth. Symbols are indicated in key. Data are in Tables 1, 2, 5, and 6. Gas sample values from Sites 991, 993, 994, 995, and 997 (small squares), sedimentary organic carbon from Sites 994, 995, and 997 (cross filling square); and DIC from Sites 994, 995, and 997 (smaller squares) are also plotted in Figure 2 for comparison. The range of $\delta^{13}C_{CH_4}$ values for Site 996 is indicated by the shaded pattern showing enrichment in $\delta^{13}C$ compared with values from a similar depth at other sites on the Blake Ridge. Similarly, the shallowest (<10 mbsf) DIC $\delta^{13}C$ values (within gray-shaded oval), are unusually ^{13}C depleted for their depth compared with the data from Sites 994, 995, and 997 (indicated by dashed line).

values more negative than –61‰ and previously reported methane to ethane ratios show a mean value of ~10,000 with a range of 700–39,000 (Paull, Matsumoto, Wallace, et al., 1996). These values are similar to those measured at Site 533 (Brooks et al., 1983) and consistent with CH_4 of microbial origin (Fig. 4). The range and mean values of both CH_4 $\delta^{13}C$ (–101.3‰ to –61.1‰; –68.4‰ ± 7.0‰) and δD (–256‰ to –136‰; –187‰ ± 20‰) (Fig. 5) are also consistent with the range of values characteristically associated with CH_4 produced via CO_2 reduction (Whiticar et al., 1986).

The causes of variation in ethane $\delta^{13}C$ values are not well established for biogenic gas deposits (Schoell, 1983), in part because ethane by definition comprises less than 0.1% of biogenic gas deposits (Bernard et al., 1977). However, small amounts of ethane are also produced by microbial processes (e.g., Vogel, 1982; Oremland et al., 1988). Whereas ethane $\delta^{13}C$ values typically are 5‰–10‰ enriched in ^{13}C relative to methane, they ultimately are sensitive to the available organic carbon base line. The mean $\delta^{13}C$ value of the Blake Ridge ethane is ~44‰ depleted with respect to the host organic carbon. Similar fractionation elsewhere has been interpreted as being consistent with the ethane being of microbial origin (Waseda and Didyk, 1995).

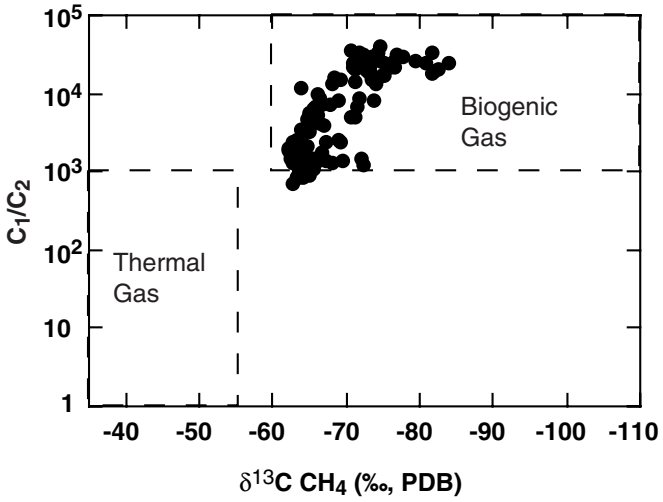

Figure 4. Plot of the methane to ethane ratios vs. the CH_4 $\delta^{13}C$ values for gas samples collected on Leg 164. Ranges that are characteristic of biogenic and thermogenic gas are indicated (after Bernard et al., 1977).

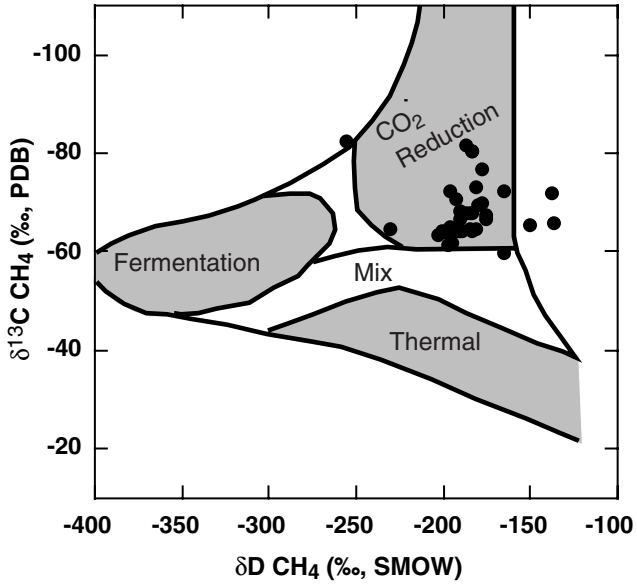

Figure 5. Crossplot of the δD vs. $\delta^{13}C$ values of CH_4 samples collected on Leg 164. Superimposed on the figure are the boundaries for the known ranges for CH_4 produced via microbial fermentation, microbial CO_2 reduction, and thermogenic processes after Whiticar et al. (1986).

Methane Isotope Variations

The broad changes in the isotopic composition of CH_4 reveal three subzones:

1. The $\delta^{13}C_{CH_4}$ values are extremely depleted at the top of the methane-bearing zone (–101‰ at –21.44 mbsf at Site 995).
2. Between 20 and 300 mbsf, the CH_4 becomes progressively more ^{13}C enriched.
3. Below 300 mbsf, the $\delta^{13}C_{CH_4}$ values are uniform (–64.0‰ ± 0.9‰).

Very negative $\delta^{13}C_{CH_4}$ values are known to occur at the top of the methane-bearing zone throughout this region and numerous other similar locations worldwide (Borowski et al., 1997). The extremely depleted $\delta^{13}C_{CH_4}$ values (e.g., ~–100‰) found near the sulfate-methane interface (SMI) are in part a response to local CH_4 recycling (Borowski et al., 1997). At the SMI, extremely ^{13}C-depleted CO_2 (i.e., –37.7‰, 20.40 mbsf, Site 995) is derived AMO. Thus, CH_4 produced from this CO_2 pool (via CO_2 reduction) will exhibit progressively larger ^{13}C depletion. Although, ^{13}C depletion extends throughout the upper ~300 mbsf, it is implausible that adequate amounts of isotopically light, recycled CH_4 produced via AMO are diffusing far enough downward, against the CH_4 concentration gradient (Dickens et al., 1997), to produce the observed $\delta^{13}C$ trend between ~30 and 300 mbsf.

The downhole shift in the CH_4 isotope $\delta^{13}C$ values may reflect changes in the isotopic composition of the DIC pool as a consequence of CO_2 reduction. A similar pattern seen at DSDP Site 533 was interpreted to be a result of Rayleigh fractionation associated with CO_2 reduction (Claypool and Threlkeld, 1983).

Below ~300 mbsf, $\delta^{13}C_{CH_4}$ values remain nearly constant (–64.0‰ ± 0.9‰) to the bottom of the holes (700–750 mbsf). Similarly, $\delta^{13}C_{CH_4}$ values do not change throughout the holes. The uniformity in the isotopic composition of the CH_4 pool below 300 mbsf suggests that the majority of the CH_4 below this level was produced by the same process. No detectable change in the CH_4 isotope values is associated with the BSR at ~450 mbsf (Holbrook et al., 1996).

Relationship Between CH_4 and CO_2 Isotope Trends

Data from DSDP Site 533 suggests that the offset between $\delta^{13}C_{CH_4}$ values and the $\delta^{13}C$ values of DIC and CO_2 gas remain constant with depth (Galimov and Kvenvolden, 1983). However, the somewhat steeper geochemical gradients and the greater sample depths achieved during Leg 164 reveal a more complex depth relationship. Both the $\delta^{13}C$ values of CO_2 gas and DIC from Sites 994, 995, and 997 clearly decrease with depth below 160 mbsf and thus the offset between the $\delta^{13}C$ values of CH_4 and CO_2 gas (or CH_4 and DIC) also decrease with depth (Fig. 6). The difference between the isotopic composition of the CO_2 gas and CH_4 is at a maximum of ~–72‰ at 120–150 mbsf (Fig. 6). This difference is equivalent to a fractionation factor of 1.077, which is commonly observed for CH_4 in marine sediments associated with CO_2 reduction (Whiticar et al., 1986). This difference decreases with depth to ~–46‰ at the base of the section, where the fractionation factor is 1.049, still within the range of fractionation factors that have been observed for CO_2 reduction elsewhere (Whiticar et al., 1986; Whiticar, 1994). Therefore, this isotope data is consistent with CO_2 reduction being the dominant methanogenic process in these sediments.

Conflicting Microbial Interpretations

Wellsbury et al. (1997) report that sediments at Site 995 contain surprisingly large amounts of acetate at depth. Acetate concentration is low near the surface (7 µM at 0.5 mbsf) and remains low for the next few hundred meters, but starts to increase sharply below 350 mbsf reaching 15,285 µM in the deepest sample (691 mbsf). Acetate is an important substrate for several microbial processes, hence, its interstitial concentrations are generally very low because of rapid turnover.

Wellsbury et al. (1997) interpreted the acetate inventories as being a consequence of increased bacterial activity at these depths, largely because of increased temperature. Laboratory experiments show that over short time periods, acetate formation is enhanced by sediment heating. Furthermore, they implicitly assume that the elevated acetate concentrations result in increased CH_4 production.

One problem that Wellsbury et al. (1997) recognize with their interpretation is that their hypothesis predicts that a substantial contribution to the CH_4 pool should come from acetate below 350 mbsf. Traditional interpretation of the expected range of CH_4, δD, and $\delta^{13}C$ values does not indicate CH_4 production via acetate formation. In de-

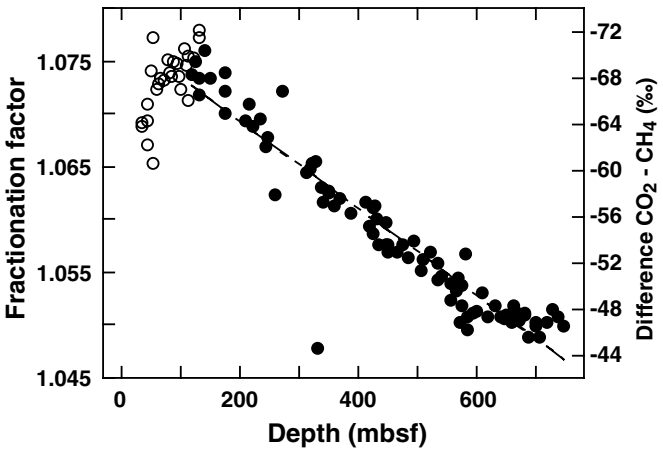

Figure 6. Plot showing both variation in the difference between coexisting CO_2 and CH_4 $\delta^{13}C$ values and the fractionation factor computed from their isotopic values vs. depth of the samples from Sites 994, 995, and 997. Closed circles are used below 120 mbsf and open circles above 120 mbsf.

fense of this, Wellsbury et al. (1997) suggest there may be "a significant deuterium exchange during acetate methanogenesis" in situ, which does occur in culture experiments (e.g., de Graaf et al., 1996). Unfortunately, it is unclear the extent to which isotopic exchange observed during inherently rapid culture experiments reflects natural systems where the processes are much slower and the reactants are limited (e.g., Burke, 1993; Sugimoto and Wada, 1995). Although the robustness of using the δD and $\delta^{13}C$ ranges to interpret the origins of the gas remains in question, we doubt that a significant shift from CH_4 production by CO_2 reduction to acetate fermentation would not result in a detectable affect in the CH_4, δD, and $\delta^{13}C$ values.

Although Wellsbury et al. (1997) were specifically discussing a different microbial population (e.g., acetate fermenters), the interpretation of increased microbial activity with depth conflicts with our data and model results. We suggest another explanation for the presence of acetate. Whereas the observed increase in acetate strongly suggests that some acetate production by microbial fermentation is continuing to occur within sediments at these burial depths, the increase in acetate concentration indicates that consumption of acetate is no longer occurring at rates sufficient to deplete the acetate pool size. Moreover, because the CH_4 in the upper ~350 mbsf does not have an isotopic composition that reflects the acetate pathway, acetate production may be a relatively insignificant process throughout this sediment column. If so, the concentration of CH_4 at depth is largely a consequence of CH_4 migration, not local production (Paull et al., 1994).

Mass Balance Considerations

Mass balance calculations indicate that the CH_4 and CO_2 reservoirs cannot be solely derived from the host sedimentary organic carbon. For example, if at 150 mbsf the CH_4 carbon (–71‰) and CO_2 carbon (–1‰) are derived from the sedimentary organic matter (–22‰) in a simple closed system, then the concentration of CH_4 should be ~30% of the total carbon gas pool. However, PCS data indicate that CH_4 comprises ~95% of the total pool (Paull, Matsumoto, Wallace, et al., 1996). Thus, the composition of the CH_4 and CO_2 pools does not balance with the available organic carbon. Therefore, additional sources and/or sinks for carbon are important.

The only clearly identified sink in these sediments that is capable of removing a significant volume of isotopically enriched carbon is authigenic siderite formation (Rodriguez et al., Chap. 30, this volume). Siderite occurs in these holes below ~150 mbsf at the 2 to 4 wt% levels and has $\delta^{13}C$ values that range between 4‰ and 11‰, with a mean value of ~+8‰ (Rodriguez et al., Chap. 30, this volume). Siderite formation does not result in significant carbon isotope fractionation. Thus, while removal of siderite carbon could produce a mass balance at ~150 mbsf, it does not help explain the smoothly varying carbon isotope profiles with depth.

Conversely, CH_4 and CO_2 migration are potentially major sources of additional carbon. The PCS data show that the total methane and CO_2 concentrations continue to increase below the base of gas hydrate stability (~450 mbsf) and remain high to the depth of the lowest successful PCS samples (560 mbsf) (Paull, Matsumoto, Wallace, et al., 1996; Dickens et al., 1997). Thus, CH_4 and CO_2 should at least be diffusing upwards along a concentration gradient from the underlying large gas reservoir.

Model Isotope Profile Simulation

A series of different isotope and mass balance models were run to simulate both closed- and open-system conditions with respect to observed $\delta^{13}C$ profiles for CH_4 and CO_2. All the models are based on initial concentrations and isotopic compositions of dissolved CH_4 (15 mM and –90‰) and CO_2 (20 mM and –22‰), like those measured at ~35 mbsf at Sites 994, 995, and 997. Changes in the isotopic composition of the carbon pools were computed using a Rayleigh fractionation model with a fractionation factor of 1.06, which is typical for CH_4 production via CO_2 reduction (Whiticar et al., 1986).

Our initial model further tested whether the concentrations and isotopic composition of the major carbon-bearing reservoirs (CH_4 and CO_2) could be derived in a closed system from CO_2 reduction (Fig. 7A). Closed-system model results failed to reproduce the observed isotopic values, concentrations, and profile curvatures. Moreover, addition of CO_2 (to simulate the DIC increase that could occur within a closed system) through organic matter decomposition (22‰) or carbonate dissolution (~0‰) does not improve model results. Previous attempts to model gas compositions from the Blake Ridge as a closed system at Site 533 also failed (Claypool and Threlkeld, 1983). Claypool and Threlkeld (1983) attributed the failure of the closed system model to the addition of gas from below.

A second model considered the consequences of adding CH_4 and CO_2, thus simulating the effect of upward gas migration through the sediment column. In this migration model, a fixed amount of CH_4 and CO_2 were added at each step, and a constant proportion of the added CO_2 was reduced to CH_4 as if by CO_2 reduction. Isotopic values were computed using a Rayleigh fractionation model (after Ussler and Paull, 1995), and isotope pool values were computed using a linear mass fraction mixing model (Gregory and Criss, 1986). This gas migration model (Fig. 7B) replicates the main characteristics seen in the upper portion of the observed CH_4-isotope profiles (Fig. 2) when increasing amounts of carbon are added and when the majority (99%) of the CO_2 is transferred to CH_4 at each step. Lower transfer efficiencies cannot reproduce the curvature and light isotopic values either. Initial model values of the CO_2 pool are also generally concordant with observed data. However, the consequence of the efficient CO_2 to CH_4 transfer is that the residual CO_2 pool becomes unrealistically enriched in ^{13}C as the model runs. Moreover, the $\delta^{13}C$ values of CO_2 and CH_4 values do not converge in this model, as they do in the observed data (Fig. 2).

A third model simulates the effects of progressive reduction in microbial activity with depth. This model is the same as the second model except the transfer efficiency was incrementally decreased to zero (Fig. 7C). Model results reasonably reproduce the observed isotopic values, concentrations, and profile curvatures (Fig. 2). The results of these models indicate that the isotopic data can be best explained as a consequence of the incremental addition of both CO_2 and CH_4, along with a progressive decrease in microbial activity with depth.

CONCLUSIONS

Measurements were made of $\delta^{13}C$ and δD on CH_4 and CO_2 gas evolved from cores, pore-water dissolved inorganic carbon

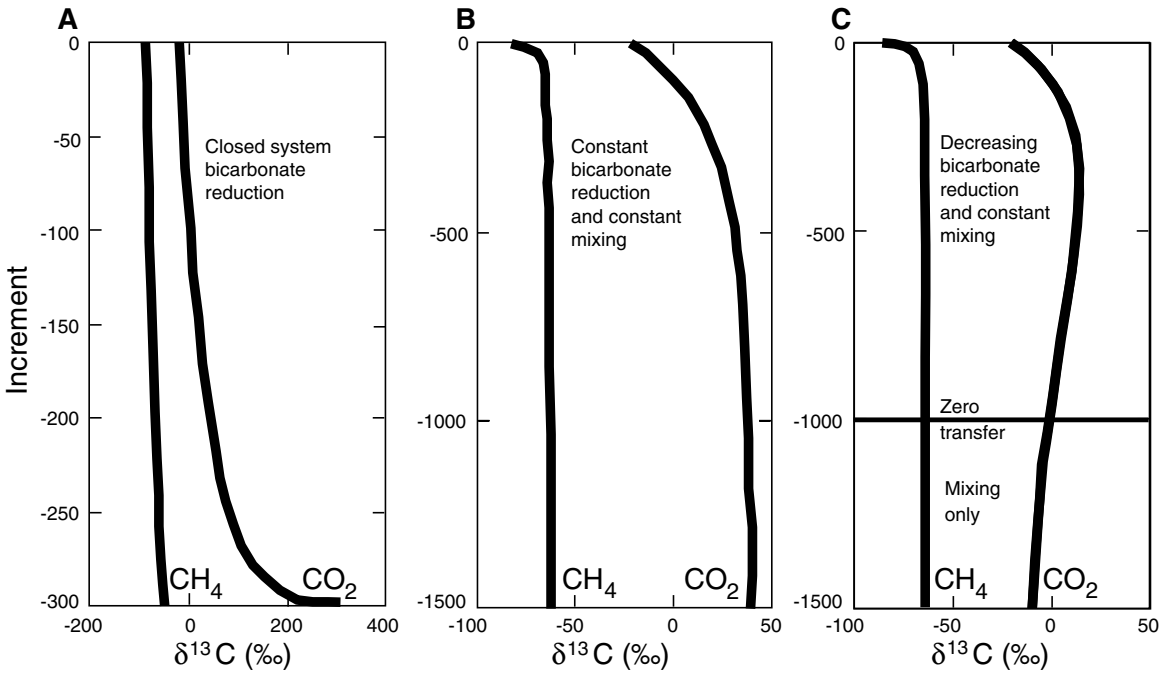

Figure 7. Computed $\delta^{13}C$ values of CH_4 and CO_2 vs. successive increments in models (**A**), (**B**), and (**C**) are shown. In (A), increments are steps in a Rayleigh fractionation ($\alpha = 1.06$) a closed system. Model steps in (B) and (C) represent stepped increments of CH_4 and CO_2 added to the system. In (B), the transfer fraction from the CO_2 pool to the CH_4 pool is constant at 0.99, and in (C), the transfer fraction decreases linearly from 0.99 at the top to 0 at the indicated level. Below this level, isotopic changes are solely due to mixing with an infinite gas reservoir. In (B) and (C), isotope values are computed using Rayleigh fractionation ($\alpha = 1.06$) and linear mass fraction mixing.

(DIC), and $\delta^{15}N$ values on sedimentary organic matter samples collected during Leg 164. Methane $\delta^{13}C$ (–68.4‰ ± 7.0‰, PDB) and δD (–187‰ ± 20‰, SMOW) values for the gases collected from Blake Ridge sediments have isotopic values characteristic of microbial CH_4 production via the CO_2 reduction pathway.

The isotopic depth profiles from three sites (Sites 994, 995, and 997) drilled along a ~10-km-long transect across the Blake Ridge are indistinguishable and show distinct depth trends in the $\delta^{13}C$ values of DIC, gaseous CO_2, and CH_4. Mean values of sedimentary organic matter ($\delta^{13}C = –22.0‰ \pm 1.4‰$, PDB; $\delta^{15}N = +5.6‰ \pm 0.7‰$, air; and C:N values = 8 ± 2) suggest that the ultimate source for the majority of the organic matter is marine. Because significant stratigraphic variation in the organic matter does not occur, variations in the organic carbon source are not a major factor in generating variations in the isotopic composition of DIC, gaseous CO_2 and CH_4. δD values of CH_4 also do not vary with depth.

Distinct variations in $\delta^{13}C$ profiles of CO_2 gas and DIC samples with depth parallel each other with an offset of 12.5‰ over the interval that they both could be sampled. Detailed shallow (<50 mbsf) DIC $\delta^{13}C$ profiles (largely from Site 995) diverge from seawater-like values to a sharply defined minimum of –37.7‰ (PDB) at the base of the sulfate-reduction zone (~20 mbsf). Collection of gaseous CO_2 requires sufficient gas evolution within the core to create gas voids. The shallowest CO_2 gas sample (34.9 mbsf; Site 997) had a $\delta^{13}C$ value of –20.6‰. With increasing depth, the $\delta^{13}C$ values of CO_2 and DIC increase to a broad maximum between 120 and 150 mbsf, where the highest values of 1.1‰ (CO_2 gas) and 10.8‰ (DIC) occur. Below ~150 mbsf, the values decrease linearly with depth.

At the top of the CH_4-bearing zone (>20 mbsf), $\delta^{13}C_{CH_4}$ values are very negative (–101.3‰, Site 995 at ~21.45 mbsf) and increase smoothly downward to a nearly constant value of –64.0‰ ± 0.9‰ below ~300 mbsf. The difference between the CH_4 and CO_2 isotopic values is not constant with depth and shows a distinct maximum between 120 and 150 mbsf. Models of how the isotopic composition of the CO_2 gas (or DIC), CH_4, and host organic carbon in these sediments change with depth indicate that a closed system with respect to carbon has not occurred during diagenesis. The models require that the CH_4 and CO_2 pools are decoupled from each other. Open-system models where the majority of CH_4 and CO_2 (>90%) are added into the system from below, and where the extent of the microbial activity decreases with depth, fit the data well. Thus, the high concentrations of CH_4 and CO_2 at Sites 994, 995, and 997 are interpreted to result from migration of CH_4 and CO_2 from depth rather than local production.

The isotopic stratigraphies at Site 996 (located at a fault conduit over the Blake Ridge Diapir) differ from all other Leg 164 sites. DIC $\delta^{13}C$ values as light as –45‰ at 3.96 mbsf suggest that the carbon was derived from methane. Here, upward advection of CH_4 and increased amounts of anaerobic methane oxidation near the seafloor where seawater sulfate is encountered dramatically affect the isotopic composition of the CO_2 pool in the top 10 mbsf.

ACKNOWLEDGMENTS

Special thanks to all those who sailed aboard the *JOIDES Resolution* on Leg 164. Howard Mendlovitz and Neil Blair made the isotopic measurements. Funding came from JOI-USSAC. Keith Kvenvolden provided a constructive review.

REFERENCES

Anderson, T.F. and Arthur, M.A., 1983. Stable isotopes of oxygen and carbon and their applications to sedimentologic and paleoenvironmental problems. *In* Arthur, M.A., Anderson, T.F., Kaplan, I.F., Veizer, J., and Land, L.S. (Eds.), *Stable Isotopes in Sedimentary Geology.* SEPM Short Course, 10.

Bernard, B.B., Brooks, J.M., and Sackett, W.M., 1977. A geochemical model for the characterization of hydrocarbon gas sources in marine sediments. *Proc. Offshore Technol. Conf.*, 2934:435–438.

Borowski, W.S., Paull, C.K., and Ussler, W., III, 1997. Carbon cycling within the upper methanogenic zone of continental rise sediments: an example

from the methane-rich sediments overlying the Blake Ridge fas hydrate deposits. *Mar. Chem.,* 57:299–311.

Brooks, J.M., Bernard, L.A., Weisenburg, D.A., Kennicutt, M.C., II, and Kvenvolden, K.A., 1983. Molecular and isotopic compositions of hydrocarbons at Site 533, Deep Sea Drilling Project Leg 76. *In* Sheridan, R.E., Gradstein, F.M., et al., *Init. Repts. DSDP,* 76: Washington (U.S. Govt. Printing Office), 377–389.

Burke, R.A., Jr., 1993. Possible influence of hydrogen concentration on microbial methane stable hydrogen isotope composition. *Chemosphere*, 26:55–56.

Cifuentes, L.A, Sharp, J.H., and Fogel, M.L. 1988. Stable carbon and nitrogen isotope biogeochemistry in the Delaware estuary. *Limnol. Oceanogr.*, 33:1102–1115.

Claypool, G.E., and Kaplan, I.R., 1974. The origin and distribution of methane in marine sediments. *In* Kaplan, I.R. (Ed.), *Natural Gases in Marine Sediments:* New York (Plenum), 99–139.

Claypool, G.E., and Threlkeld, C.N., 1983. Anoxic diagenesis and methane generation in sediments of the Blake Outer Ridge, Deep Sea Drilling Project Site 533, Leg 76. *In* Sheridan, R.E., Gradstein, F.M., et al., *Init. Repts. DSDP,* 76: Washington (U.S. Govt. Printing Office), 391–402.

Coleman, M.L., Shepherd, T.J., Durham, J.J., Rouse, J.E., and Moore, G.R., 1982. Reduction of water with zinc for hydrogen isotope analysis. *Anal. Chem.,* 54:993–995.

Craig, H., 1953. The geochemistry of stable carbon isotopes. *Geochim. Cosmochim. Acta*, 3:53–92.

de Graaf, W., Wellsbury, P., Parks, R.J., and Cappenberg, T.E., 1996. Comparison of acetate turnover in methanogenic and sulfate-reducing sediments by radiolabeling and stable isotope labeling and by use of specific inhibitors: evidence for isotopic exchange. *Appl.Environ. Microbiol.*, 62:772–777.

Deines, P., 1980. The isotopic composition of reduced organic carbon. *In* Fritz, P., and Fontes, J.C. (Eds.), *Handbook of Environmental Isotope Geochemistry* (Vol. 1)*: The Terrestrial Environment, A:* Amsterdam (Elsevier), 329–406.

Dickens, G.R., Paull, C.K., Wallace, P., and the ODP Leg 164 Scientific Party, 1997. Direct measurement of in situ methane quantities in a large gas-hydrate reservoir. *Nature,* 385:427–428.

Duan, Z., Møller, N., Greenberg, J., and Weare, J.H., 1992. The prediction of methane solubility in natural waters to high ionic strengths from 0° to 250°C and from 0 to 1600 bar. *Geochim. Cosmochim. Acta,* 56:1451–1460.

Emrich, K., Ehhalt, D., and Vogel, J., 1970. Carbon isotope fractionation during the precipitation of calcium carbonate. *Earth Planet. Sci. Lett.,* 8:363–371.

Fenchel, T., and Blackburn, T.H., 1979. *Bacteria and Mineral Cycling:* London (Academic Press).

Galimov, E.M., and Kvenvolden, K.A., 1983. Concentrations of carbon isotopic compositions of CH_4 and CO_2 in gas from sediments of the Blake Outer Ridge, Deep Sea Drilling Project Leg 76. *In* Sheridan R.E., Gradstein, F.M., et al., *Init. Repts. DSDP,* 76: Washington (U.S. Govt. Printing Office), 403–407.

Gradstein, F.M., and Sheridan, R.E., 1983. Introduction. *In* Sheridan R.E., Gradstein, F.M., et al., *Init. Repts. DSDP,* 76: Washington (U.S. Govt. Printing Office), 5–18.

Gregory, R.T., and Criss, R.E., 1986. Isotopic exchange in open and closed systems. *In* Valley, J.W., Taylor, H.P., Jr., and O'Neil, J.R. (Eds.), *Stable Isotopes in High Temperature Geological Processes.* Mineral. Soc. Am., Reviews in Mineralogy, 16:91–127.

Hedges, J.I., and Stern, J.H., 1984. Carbon and nitrogen determinations of carbonate-containing solids. *Limnol. Oceanogr.*, 29:657–663.

Holbrook, W.S., Hoskins, H., Wood, W.T., Stephen, R.A., Lizzarralde, D., and the Leg 164 Science Party, 1996. Methane gas-hydrate and free gas on the Blake Ridge from vertical seismic profiling. *Science,* 273:1840–1843.

Kendall, C., and Coplen, T.B., 1985. Multisample conversion of water to hydrogen by zinc for stable isotope determination. *Anal. Chem.,* 57:1437–1440.

Martens, C.S., and Berner, R.A., 1974. Methane production in the interstitial waters of sulfate-depleted marine sediments. *Science*, 185:1167–1169.

Merritt, D.A., and Hayes, J.M., 1995. Carbon isotopic analysis of atmospheric methane by isotope-ratio-monitoring gas chromatography-mass spectrometry. *J.Geophys Res.*, 100:1317–1326.

Meyers, P.A., 1994. Preservation of elemental and isotopic source identification of sedimentary organic matter. *Chem. Geol.,* 144:289–302.

Olsen, K., 1997. Measurement of the $\delta^{13}C$ (org) and $\delta^{15}N$ (org) in sediments of the Blake Ridge, Ocean Drilling Program Leg 164 [Senior thesis]. Univ. of North Carolina, Chapel Hill, NC.

Oremland, R.S., Whiticar, M.J., Strohmaier, F.E., and Kiene, R.P., 1988. Bacterial ethane formation from reduced, ethylated sulfur compounds in anoxic sediments. *Geochim. Cosmochim. Acta,* 52:1895–1904.

Paull, C.K., Matsumoto, R., Wallace, P.J., et al., 1996. *Proc. ODP, Init. Repts.,* 164: College Station, TX (Ocean Drilling Program).

Paull, C.K., Ussler, W., III, and Borowski, W.A., 1994. Sources of biogenic methane to form marine gas-hydrates: in situ production or upward migration? *Ann. N.Y. Acad. Sci.,* 715:392–409.

Popp, B.N., Sansone, F., Francis, F.J., and Rust, T.M., 1995. Determination of concentration and carbon isotopic composition of dissolved methane in sediments and nearshore waters. *Anal. Chem.*, 67:405–411.

Presley, B.J., and Kaplan, I.R., 1968. Changes in dissolved sulfate, calcium and carbonate from interstitial water of near shore sediments. *Geochim. Cosmochim. Acta,* 32:1037–1049.

Reeburgh, W.S., 1976. Methane consumption in Cariaco Trench waters and sediments. *Earth Planet. Sci. Lett.,* 28:337–344.

————, 1980. Anaerobic methane oxidation: rate depth distribution in Skan Bay sediments. *Earth Planet. Sci. Lett.,* 47:345–352.

Rosenfeld, W.D., and Silverman, S.R., 1959. Carbon isotope fractionation in bacterial production of methane. *Science,* 130:1658–1659.

Schoell, M., 1980. The hydrogen and carbon isotopic composition of methane from natural gases of various origins. *Geochim. Cosmochim. Acta,* 44:649–661.

————, 1983. Genetic characterization of natural gases. *AAPG Bull.*, 67:2225–2238.

Shipboard Scientific Party, 1972. Sites 102-103-104—Blake-Bahama Outer Ridge (northern end). *In* Hollister, C.D., Ewing, J.I., et al., *Init. Repts. DSDP,* 11: Washington (U.S. Govt. Printing Office), 135–218.

Sugimoto, A., and Wada, E., 1995. Hydrogen isotopic composition of bacterial methane: CO_2/H_2 reduction and acetate fermentation. *Geochim. Cosmochim. Acta*, 59:1329–1337.

Tissot, B.P., and Welte, D.H., 1984. *Petroleum Formation and Occurrence* (2nd ed.): Heidelberg (Springer-Verlag).

Ussler, W., III, and Paull, C.K., 1995. Effects of ion exclusion and isotopic fractionation on pore water geochemistry during gas hydrate formation and decomposition. *Geo-Mar. Lett.,* 15:37–44.

Vogel, T.M., Oremland, R.S., and Kvenvolden, K.A., 1982. Low-temperature formation of hydrocarbon gases in San Francisco Bay sediment (California). *Chem. Geol.,* 37:289–298.

Wahlen, M., 1993. The global methane cycle. *Annu. Rev. Earth Planet. Sci.*, 21:407–426.

Waseda, A., and Didyk, B.M., 1995. Isotope compositions of gases in sediments from the Chile continental margin. *In* Lewis, S.D., Behrmann, J.H., Musgrave, R.J., and Candy, S.C., (Eds.), *Proc. ODP, Sci. Results*, 141: College Station, TX (Ocean Drilling Program), 307–312.

Weiss, R.F., 1974. Carbon dioxide in water and seawater: the solubility of a non-ideal gas. *Mar. Chem.*, 2:203–215.

Wellsbury, P., Goodman, K., Barth, T., Cragg, B.A., Barnes, S.P., and Parkes, R.J., 1997. Deep marine biosphere fueled by increasing organic matter availability during burial and heating. *Nature,* 388:573–576.

Whiticar, M.J., 1994. Correlation of natural gases with their source. *In* Magoon, L.B., and Dow, W.G. (Eds.), *The Petroleum System—From Source to Trap*. AAPG Mem., 60:261–283.

Whiticar, M.J., Faber, E., and Schoell, M., 1986. Biogenic methane formation in marine and freshwater environments: CO_2 reduction vs. acetate fermentation—isotope evidence. *Geochim. Cosmochim. Acta,* 50:693–709.

Date of initial receipt: 30 April 1998
Date of acceptance: 12 January 1999
Ms 164SR-207